

Phase Equilibria and Crystal Growth for LiREF₄ Scheelite Crystals

Detlef Klimm¹, Ivanildo A. dos Santos², Izilda M. Ranieri², and Sonia L. Baldochi²

¹Leibniz Institute for Crystal Growth, Max-Born-Str. 2, 12489 Berlin, Germany

²Center for Lasers and Applications, IPEN, Butantã 05422-970, São Paulo, SP, Brazil

ABSTRACT

The scheelite type laser crystals LiREF₄ melt congruently only for RE being one of the elements Er, Tm, Yb, Lu, or possibly Y, respectively. For RE = Eu, Gd, Tb, Dy, or Ho the corresponding scheelites undergo a peritectic melting under the formation of the corresponding rare earth fluoride. The melting behavior of LiREF₄ mixed crystals with two or more RE is not yet known well. If RE is a mixture of Gd and Lu, Gd rich solid solutions melt peritectically under formation of (Gd,Lu)F₃ and Lu rich solid solutions melt directly without formation of other solid phases.

INTRODUCTION

Most of the binary systems LiF–REF₃, where RE is one of the rare earth elements from lanthanum to lutetium, or yttrium, respectively, were described by Thoma [1]. For the smaller rare earth ions, starting from RE = Eu, the systems contain one intermediate phase LiREF₄ that crystallizes at ambient conditions in the scheelite structure. At high pressure (10.7 GPa in the case of LiLuF₄ [2]) a reversible phase transformation to a monoclinic phase is observed for the smaller RE, contrary the scheelites decompose under formation of RE rich phases and LiF for the larger RE (beyond 11 GPa in the case of LiGdF₄ [3]). Solid state synthesis and lattice parameters for these compounds were reported by Keller and Schmutz [4]. The thermal stability of the scheelites under ambient pressure is larger for the smaller RE³⁺. LiEuF₄ is stable up to 690°C where it decomposes peritectically under the formation of β-EuF₃. Peritectic decomposition to a melt and the low-*T* (β-) phase of the REF₃ is also observed for RE = Gd, Tb, Dy, Ho, and Y; but the peritectic point shifts in this sequence closer to the solidus of the LiREF₄ phase. LiErF₄ is controversially reported to melt incongruently [5] or congruently [1]. If one assumes a smooth variation of the melting temperatures *T_f* for neighboring RE, congruent melting seems more realistic, since LiTmF₄, LiYbF₄, and LiLuF₄ melt congruently [1]. Recently from a DFT evaluation structural parameters *a*₀, *c*₀, elastic stiffness coefficients *c_{ij}*, and thermodynamic parameters were derived for most of the LiREF₄ [6]. It was concluded that the scheelite structure should be stable also for the large RE from Pm to Ce, but the energies for the LiREF₄ from Gd to Lu are more favorable, which is in reasonable agreement with the experimental phase diagrams [1].

The LiREF₄ scheelites attract not only academic interest as some of them are interesting laser host materials where the host RE³⁺ can be replaced by another rare earth laser ion RE³⁺. LiYF₄ (YLF), often doped with Nd, is a good example that is offered by several suppliers commercially. YLF crystals can be grown from melts with slight LiF excess (molar fraction *x_Y*=0.48) e.g. by the Czochralski or Bridgman technique [7,8]. The fluoride crystals are sensitive against hydrolysis during growth which can be suppressed e.g. by an atmosphere containing CF₄

or even HF during the Czochralski process [9]. This paper reports new and reviews recent results on phase relations and crystal growth within binary $\text{LiREF}_4\text{-LiRE}'\text{F}_4$ systems.

EXPERIMENT

LiF (Aldrich, 99.9% = 3N purity) was zone melted for purification in a platinum boat (cross section 1 cm^2 , length 20 cm) inside a platinum tube that was rinsed by a HF/Ar mixture. REF_3 (RE = Gd, Lu, or Y) were prepared from commercial RE_2O_3 (typically 3N–5N purity) by hydrofluorination at 850°C in the same apparatus. This process is described in detail elsewhere [10]. Conversion rates $>99.9\%$ of the theoretical value calculated for the reaction $\text{RE}_2\text{O}_3 + 6\text{HF} \rightarrow 2\text{REF}_3 + 3\text{H}_2\text{O}$ were measured by comparing the masses prior to and after the hydrofluorination process. The samples were mainly prepared by melting and slow cooling (15 K/hour) under HF/Ar. Only for LiLuF_4 and LiGdF_4 pieces from Czochralski grown single crystals were used. It will be shown later that the melting behavior of most LiREF_4 mixed crystals can only be described, if the phase relations of REF_3 mixed crystals are known and consequently some of these system were studied first.

Three different NETZSCH simultaneous DTA/TG or DSC/TG equipments were used for thermal analysis: The systems $\text{REF}_3\text{-RE}'\text{F}_3$ and $\text{LiREF}_4\text{-LiRE}'\text{F}_4$ were investigated using a STA 449C (Pt/Rh furnace, DSC sample holder, graphite or Pt crucibles) and a STA 409CD (graphite furnace, DTA sample holder, graphite crucibles) or a STA 409 PC/PG (SiC furnace, DSC sample holder, Pt crucibles). The crucibles were covered with lids. After evacuation of the thermal analyzers the samples were measured in flowing Ar (99.999% purity) with a heating rate of 10 K/min. Such procedure could avoid hydrolysis of the sensitive fluorides almost completely.

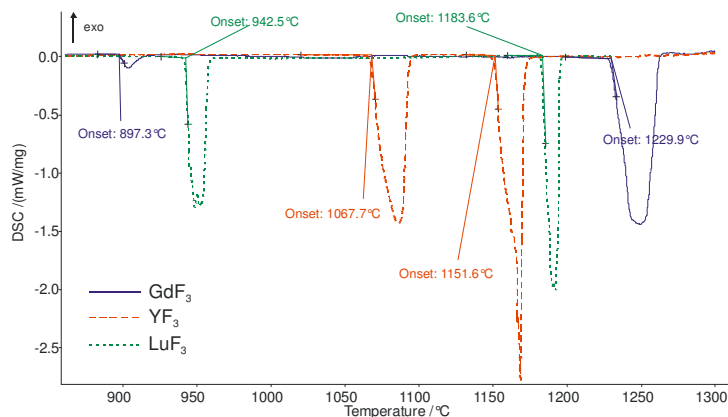


Fig. 1: DSC curves (2nd heating run, original data without smoothing) of pure REF_3 showing subsequently peaks from the phase transformation (T_t) and from melting (T_f).

Usually only heating curves were used for the construction of phase diagrams, as cooling curves did often show supercooling. A typical example for GdF_3 , YF_3 , and LuF_3 is shown in Fig. 1. Powder samples ($\approx 10\ \mu\text{m}$ grains) with masses around 20 mg as obtained from the hydrofluorination process were used for these measurements. The 2nd heating curves that are shown in Fig. 1 do not differ remarkably from the 1st heating curves that were obtained with the initial powders. After the DSC runs the molten and solidified samples formed one drop on the bottom of the crucible. The small mass loss (not shown in the figure, but never exceeding 4%; $<1\%$ are typical) during these measurements and mainly well shaped sharp peaks prove that the samples and the gas flow in the thermal analyzer were free from oxygen and humidity. It is

obvious that all three REF_3 show two subsequent thermal effects: A first endothermal peak at T_t indicates a first order solid state phase transformation and a second endothermal peak at T_f indicates melting. Similar measurements were performed with binary mixtures $\text{GdF}_3\text{--YF}_3$ [11] and $\text{GdF}_3\text{--LuF}_3$ [12].

As expected, both peaks become broader for intermediate compositions because phase transformation as well as melting take place in a temperature interval instead of a fixed T for solid solutions. In the case of $\text{GdF}_3\text{--YF}_3$, it was found that the onset of the phase transformation peak changes almost continuously from $T_t \approx 900^\circ\text{C}$ (GdF_3) to $T_t \approx 1066^\circ\text{C}$ (YF_3), passing a weak maximum around 10% GdF_3 where T_t reaches 1080°C . (All concentrations throughout the text are given in mol-%). The melting point changes also continuously from $T_f \approx 1230\text{--}1250^\circ\text{C}$ (GdF_3) to $T_f \approx 1130\text{--}1150^\circ\text{C}$ (YF_3), passing a weak minimum around 25% GdF_3 where T_f reaches 1120°C [11].

Conversely, $\text{GdF}_3\text{--LuF}_3$ mixtures show a different behavior: Here T_t rises from both sides ($\approx 900^\circ\text{C}$ or $\approx 945^\circ\text{C}$, respectively) and reaches a constant value $T_t \approx 1051^\circ\text{C}$ for intermediate compositions from 20 to 60% LuF_3 . Instead, T_f drops from both sides (1250°C or 1182°C , respectively) to a constant eutectic temperature $T_{\text{eut}} = 1092^\circ\text{C}$ that can be observed for compositions between 20 and 70% LuF_3 . Moreover, nine $\text{GdF}_3\text{--LuF}_3$ samples with different composition were pulverized and lattice constants were measured using a Bruker AXS diffractometer. The diffraction patterns could be fitted satisfactory to the $Pnma$ space group and no parasitic peaks indicating other phases were found [12].

As written above, most LiF--REF_3 phase diagrams are already published [1], and only the system LiF--GdF_3 was re-determined recently [13]. For practical applications the scheelites LiREF_4 (usually doped with another RE') are the most interesting phases within these systems, but the knowledge on pseudo-binary systems $\text{LiREF}_4\text{--LiRE}'\text{F}_4$ is scarce. DSC results on LiGdF_4 , LiLuF_4 , and their binary mixtures were published in a previous paper [14].

A single mixed crystal was grown from the composition $\text{Li}(\text{Lu}_{0.75}\text{Gd}_{0.25})\text{F}_4$ by the Czochralski method under high purity $\text{CF}_4 + \text{Ar}$ atmosphere, in a commercial system with automated diameter control. The crystal was pulled with a growth rate of 1 mm/hour and a rotation rate of 15 rpm for a [100] oriented boule, a seed of LiLuF_4 was used to achieve the crystallization process. The crystal with 50 mm in length, 15 mm in diameter and 52 g is shown in Fig. 2. The crystal is optically clear and grew well.



Fig. 2: Czochralski grown scheelite mixed crystal $\text{Li}(\text{Lu}_{0.75}\text{Gd}_{0.25})\text{F}_4$.

DISCUSSION

The concentration triangle $\text{LiF--GdF}_3\text{--LuF}_3$ shall be used as an example for the discussion of phase equilibria that are relevant for the growth of scheelite mixed crystals. The scheelites can be found on the dashed line in Fig. 3.

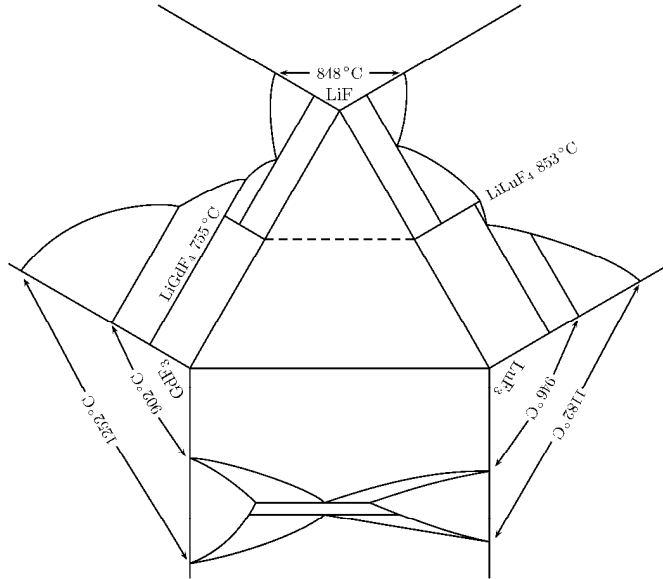


Fig. 3: Concentration triangle LiF–GdF₃–LuF₃ with intermediate scheelites LiGdF₄ (incongruently melting) and LiLuF₄ (congruently melting)

It should be noted that binary subsystems in phase diagrams can only be spanned between compounds with congruent melting behavior. This is a necessary, but not sufficient condition, and this condition is fulfilled only for a few RE-RE' pairs. In Fig. 3, only LiLuF₄ shows congruent melting, whereas LiGdF₄ melts incongruently. Besides LiLuF₄, the LiREF₄ scheelites with RE = Yb, Tm, Er show congruent melting behavior too. LiYF₄ is arguable, as the temperature of its solidus is at least so close to the liquidus at this composition that they cannot be resolved by means of thermal analysis. All other LiREF₄ undergo a peritectic decomposition to a melt and remaining REF₃ in the low-*T* phase, which is for all rare earth fluorides the β-YF₃ type. From the data that are given in Tab. 1 it becomes obvious that at least for the melting of pure LiREF₄ never the formation of the high-*T* REF₃ phase has to be taken in account.

RE	Eu	Gd	Tb	Dy	Ho	Y	Er	Tm	Yb	Lu
LiREF ₄ melting	690 per.	755 per.	787 per.	819 per.	799 per.	812 con.?	832 con.	785 con.	790 con.	794 con.
LiREF ₄ liquidus	763	857	842	843	819	≈812	832	785	790	794
REF ₃ low- <i>T</i>	β-YF ₃ type									
<i>T</i> _t	765	878	998	1082	1100	1059	1101	1044	949	937
REF ₃ high- <i>T</i>	tysonite type						α-UO ₃ type			

Tab. 1: Melting temperature and melting behavior for the known LiREF₄ scheelites, together with the corresponding solid state phase transformation temperatures *T*_t of the corresponding REF₃ and their structure types below and above *T*_t (temperatures in °C).

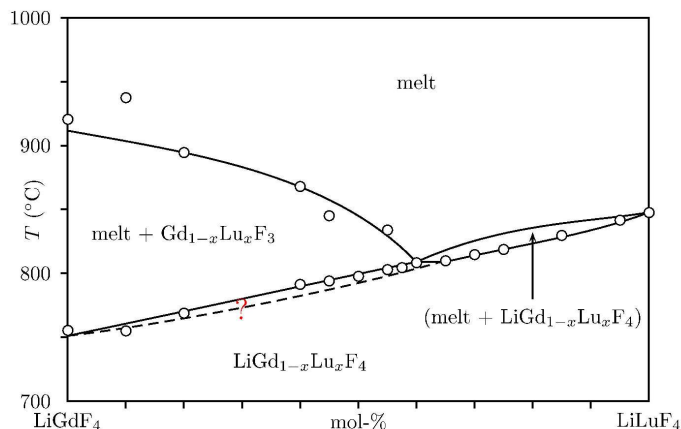


Fig. 4: The tentative scheelite section (dashed line in Fig. 3) showing peritectic decomposition scheelite \rightarrow melt + (Gd,Lu) F_3 for LiGd F_4 rich compositions and incongruent melting for LiLu F_4 rich compositions [14].

As mentioned above, pseudo-binary phase diagrams can be constructed between the congruently melting LiREF $_4$, this means for RE, RE' = {Lu, Yb, Tm, Er, and possibly Y}. To the author's knowledge, none of these $(5 \times 4) / 2 = 10$ pseudo-binary systems was measured up to now. However, the scheelite section LiGdF $_4$ -LiLuF $_4$ of the ternary system LiF-GdF $_3$ -LuF $_3$ was investigated recently [14], and it was found that for compositions close to LiGdF $_4$ (<60 mol-% LiLuF $_4$) the mixed crystal scheelite decomposes peritectically to (Gd,Lu) F_3 and melt, whereas LiLuF $_4$ rich compositions melt directly, without peritectic decomposition (Fig. 4). It should be noted, however, that a mixed crystal usually not melts congruently: Congruent melting would mean that a solid body and a liquid phase with identical chemical composition are in equilibrium. This is for mixed crystals the case only at azeotropic points where liquidus and solidus have one common maximum (e.g. SrNb $_2$ O $_6$ -BaNb $_2$ O $_6$ [15]) or minimum (e.g. CaF $_2$ -SrF $_2$ [16]), and such azeotropic point does not occur at least in Fig. 4.

CONCLUSIONS

The melting and crystallization behavior of scheelite type LiREF $_4$ mixed crystals, where the rare earth element is partially substituted by another RE', can in most cases only be described in terms of ternary phase diagrams. Only if both rare earth elements belong to the set {Lu, Yb, Tm, Er, and possibly Y}, it can be expected that the scheelite mixed crystals behave as binary mixtures.

The 2-phase-field "melt+scheelite" is, at least for RE, RE' = Gd, Lu, very narrow, resulting in a segregation coefficients of both rare earth elements during crystal growth that are close to unity. Consequently, the melt growth of single crystals with good homogeneity is possible outside the composition region where peritectic decomposition of the scheelite to a melt and rare earth fluoride mixed crystal takes place. A similar narrow separation between liquidus and solidus of scheelite mixed crystal was reported by Abell et al. [17] for the system LiYF $_4$ -LiErF $_4$ where both end members melt congruently and homogeneous crystals Li(Y,Er)F $_4$ without segregation could be grown. It should be noted, however, that Y $^{3+}$ and Er $^{3+}$ have almost identical ionic radii (104 or 103 pm, respectively for octahedral coordination, Shannon) compared with Gd $^{3+}$ and Lu $^{3+}$ (107.8 or 100.1 pm, respectively) — but the larger difference of the pair Gd $^{3+}$ -Lu $^{3+}$ does not influence the melting behavior considerably.

ACKNOWLEDGMENTS

The authors express their gratitude to “Coordenação de Aperfeiçoamento de Pessoal de Nível Superior” (CAPES) and to “Deutscher Akademischer Austauschdienst” (DAAD) for financial support.

REFERENCES

1. R. E. Thoma, in *Prog. Sci. Technol. Rare Earths*, Vol. 2 (Pergamon Press, New York, 1966) pp. 90-122.
2. A. Grzechnik, K. Friese, V. Dmitriev, H.-P. Weber, J.-Y. Gesland, W. A. Crichton, *J. Phys.: Condens. Matter* **17**, 763 (2005).
3. A. Grzechnik, W. A. Crichton, P. Bouvier, V. Dmitriev, H.-P. Weber, J.-Y. Gesland, *J. Phys.: Condens. Matter* **16**, 7779 (2004).
4. C. Keller and H. Schmutz, *J. Inorg. Nucl. Chem.* **27**, 900 (1965).
5. I. A. Ivanova, M. A. Petrova, I. G. Podkolzina, *Z. Neorg. Chim.* **20**, 2292 (1975).
6. B. Minisini, P. Bonnaud, Q. A. Wang, F. Tsobnang, *Comp. Mat. Sci.* **42**, 156 (2008).
7. W. A. Shand, *J. Crystal Growth* **5**, 143 (1969).
8. G.J. Quarles, L. Esterowitz, G. M. Rosenblat, R. Uhrin, R. F. Belt. In: *OSA Proc. on Advances Solids State Laser* **13**, 306 (1993).
9. M. Louis, E. Simoni, S. Hubert, J. Y. Gesland, *Optical Materials* **4**, 657 (1995).
10. H. Guggenheim, *J. Appl. Phys.* **34**, 2482 (1963).
11. D. Klimm, I. M. Ranieri, R. Bertram, S. L. Baldochi, *Mat. Res. Bull.* **43**, 676 (2008).
12. I. M. Ranieri, S. L. Baldochi, D. Klimm, *J. Solid State Chem.* **181**, 1070 (2008).
13. I. M. Ranieri, A. H. A. Bressiani, S. P. Morato, S. L. Baldochi, *J. Alloys. Comp.* **379**, 95 (2004).
14. I. A. dos Santos, I. M. Ranieri, D. Klimm, R. Fornari, S. L. Baldochi, *Cryst. Res. Technol.* **43**, 1168 (2008).
15. J. R. Carruthers, M. Grasso, *J. Electrochem. Soc.* **117**, 1426 (1970).
16. D. Klimm, M. Rabe, R. Bertram, R. Uecker, L. Parthier, *J. Crystal Growth* **310**, 152 (2008).
17. J. S. Abell, I. R. Harris, B. Cockayne, *J. Mat. Sci.* **12**, 670 (1977).